



#### Available online at www.sciencedirect.com

## **ScienceDirect**

Procedia Procedia

Energy Procedia 63 (2014) 911 - 925

## GHGT-12

# Predicting Aerosol Based Emissions in a Post Combustion CO<sub>2</sub> Capture Process Using an Aspen Plus Model

Purvil Khakharia<sup>a</sup>\*, Jan Mertens<sup>b</sup>, Thijs J.H. Vlugt<sup>c</sup>, Earl Goetheer<sup>a</sup>

<sup>a</sup>TNO, Leeghwaterstraat 46, 2628 CA, Delft, The Netherlands
<sup>b</sup>Laborelec, Rodestraat 125, 1630 Linkebeek, Belgium
<sup>c</sup>TU Delft, Leeghwaterstraat 39,2628 CB, Delft, The Netherlands

#### Abstract

Industrial scale implementation of post combustion CO<sub>2</sub> capture (PCCC) can be hindered by solvent emissions due to its impact on the environment and the operating costs. The issue of aerosol based emissions has only been recently reported for a PCCC process and very little fundamental knowledge is available in the scientific community on this topic. Therefore, it is important to understand the mechanism of aerosol formation and growth so that appropriate countermeasures can be applied in reducing the total emissions. In this study, a simplified methodology is presented for predicting aerosol based emissions from a CO<sub>2</sub> capture column of a PCCC process. The basis of this methodology is to split the counter-current gas-liquid interaction from the cocurrent gas-aerosol interaction. The absorption column is discretised into multiple alternating gas-liquid and gas-aerosol sections in Aspen Plus with an assumption that aerosols behave as a continuous phase rather droplets. The degree of supersaturation, which is important for aerosol formation and growth, is calculated along the column. The effect of the changes in parameters of the PCCC plant, such as the CO<sub>2</sub> content of the inlet flue gas, the lean solvent temperature and the lean solvent loading on aerosol based emissions are investigated. The aerosol based emissions follows the trend of the supersaturation ratio in the absorber column.

© 2014 Published by Elsevier Ltd. This is an open access article under the CC BY-NC-ND license (http://creativecommons.org/licenses/by-nc-nd/3.0/).

Peer-review under responsibility of the Organizing Committee of GHGT-12

\* Corresponding author. Tel.: +31888664543 *E-mail address*: purvil.khakharia@tno.nl

doi:10.1016/j.egypro.2014.11.101

Keywords: Post Combustion CO<sub>2</sub> capture, Aerosol, Supersaturation, Modelling, Reactive Absorption

#### 1. Introduction

Climate change and in particular, temperature rise is a major issue of the current century (Abunowara and Elgarni, 2013; Mori et al., 2013). Greenhouse gases, especially carbon dioxide (CO<sub>2</sub>), emitted from anthropogenic sources like fossil fuel based power plants are a major cause for climate change (Aaheim et al., 1999; Abunowara and Elgarni, 2013; Min et al., 2011). Carbon capture and storage (CCS) is globally under extensive research and development to reduce CO<sub>2</sub> emission in the atmosphere (Wall, 2007). An absorption-desorption based Post Combustion CO<sub>2</sub> Capture (PCCC) process is one of the most mature and promising technology for capturing the CO<sub>2</sub> emitted from large point sources like fossil fuel based power plants (Abu Zahra, 2009; MacDowell et al., 2010; Rochelle, 2009; Sanchez-Fernandez et al., 2013).

A 30 wt.% aqueous Monoethanolamine (MEA) solution can be considered as the state of the art solvent for a typical PCCC process (Abu Zahra, 2009; Alie et al., 2005; Rao and Rubin, 2002). The entire process is highly energy demanding and reduces the overall power plant efficiency up to 12 % points (Abu Zahra, 2009). Apart from energy losses, amine losses due to emissions, thermal degradation and oxidative degradation are a major concern as these not only increase the operating cost, but also lead to adverse environmental effects (IEAGHG, 2010; Mertens et al., 2012). There are two types of solvent losses due to emissions: (1) emissions due to the component's volatility (vapour emission); and (2) emissions due to aerosols (aerosol emission) (Schaber, 1994). Here the word 'aerosols' refers to 'aerosol droplets'. Solvent loss by means of mechanical entrainment can be easily controlled and therefore, not considered to occur in PCCC.

The amount of vapour emissions is (amongst others), a function of the volatility of the amine, loading of the solvent and the temperature of the gas phase (da Silva et al., 2013; Nguyen et al., 2011). A number of studies (both experimental and theoretical) have been carried out to understand volatility based solvent emissions from PCCC plants (Mertens et al., 2012; Nguyen et al., 2011, 2010; Trollebø et al., 2013, Khakharia et al., 2014b). To reduce vapour emissions, the use of a water wash at the top of the absorber column has shown to be effective (da Silva et al., 2013). MEA emissions of about 1.4 mg/Nm³ in the treated flue gas stream after water wash can be achieved (de Koeijer et al., 2011). However, the water wash section at the top of the absorber column is ineffective in controlling aerosol based emissions (da Silva et al., 2013; Gretscher and Schaber, 1999, Mertens et al., 2013). Aerosol based emissions from a PCCC process can be in the order of several grams per Nm³ (da Silva et al., 2013; Khakharia et al., 2013, 2014a).

The mechanism of aerosol formation and growth is related to the degree of supersaturation. The degree of supersaturation of flue gas (S) can be calculated using the following equation;

$$S = \frac{P_C(T, y_1, y_2 \dots y_n)}{P_{CS}(T, y_1, y_2 \dots y_n)}$$
 Eq. (1)

where  $P_C$  is the total partial pressure of all condensing vapour component at the actual temperature T and mole fraction,  $y_i$  of the supersaturated gas, and  $P_{CS}$  is the total partial pressure of all the condensing components corresponding to the phase equilibrium (Gretscher and Schaber, 1999).

If the supersaturation exceeds a critical value, nucleation takes places and nuclei are formed by molecules of condensing components (homogeneous nucleation) and/or on the impurities in the flue gas (heterogeneous nucleation). Heterogeneous nucleation is induced at low supersaturation ratio ( $S \sim 1$ ) whereas, homogeneous nucleation occurs at higher supersaturation ratio (S > 2) (Gretscher and Schaber, 1999; Schaber, 1994). Heterogeneous nuclei present in the flue gas entering the absorber could be for instance sulphuric acid aerosols. Flue gas leaving the flue gas desulphurisation unit of typical coal fired power plant has been reported to have  $H_2SO_4$  concentration in the range of 1 to 12 parts per million (ppm) equivalent of  $SO_3$  (Wattanaphan et al., 2013). The

presence of impurities like  $H_2SO_4$  in the flue gas can initiate heterogeneous nucleation even at very low supersaturation (Gretscher and Schaber, 1999). The relation of the  $H_2SO_4$  aerosols and the corresponding particle number concentration to the emissions of the solvent has been proved in a previous study (Khakharia et al., 2013).

Understanding and modelling of vapour emissions is relatively straight forward (da Silva et al., 2013; Nguyen et al., 2011, 2010). Aerosol based emission is a more complex phenomena to model and to predict. However, modelling is an indispensable tool to understand the complex mechanism and predict the extent of aerosol based emissions. The developed model should be accurate and at the same time be robust. As a first step, this study presents a simplified modelling approach to predict aerosol emission as a function of the operating conditions. The methodology is implemented in Aspen Plus which is a commercially available flow sheeting tool. This model is intended to serve the purpose of understanding and predicting trends. The modelling tool is an approximation and the exact local conditions within the plant can differ. Hence, it should be noted that values reported can only be compared qualitatively with experimental results.

## Nomenclature

CCS Carbon Capture and Storage PCCC Post Combustion CO<sub>2</sub> Capture

MEA Monoethanolamine PFR Plug Flow Reactor

## 2. Modeling approach and assumptions

## 2.1. Methodology

To model a CO<sub>2</sub> absorption column, mass and heat transfer processes occurring in each of the phase need to be solved simultaneously. However, standard flowsheeting tools such as Aspen Plus do not have the option of introducing an additional phase in an absorption column. Therefore, in this study a simplified modelling approach was used to understand aerosol based emissions in a reactive absorption process using standard flowsheeting tools such as Aspen Plus. This is shown in Figure 1a. The absorption liquid flows counter-current to the gas phase, while the aerosol phase is co-current to the gas phase. The absorber column is divided into smaller sections and instead of the simultaneous mass and heat transfer process of all the three phases, the process is divided into two steps. The first step is the counter-current contact between liquid and gas phase. The second step is the co-current contact of aerosols with the resulting gas phase from the first step. It is assumed that there is no direct contact between the absorption liquid phase and the aerosols.

## 2.2. Implementation in Aspen Plus

The process simulation software, Aspen Plus V8.0 was used as the modelling tool. A single absorption column is divided into smaller absorber sections. Each section consist of two calculation blocks. In the first calculation block, the mass and heat transfer of the counter current gas-liquid absorption is solved using a rate based absorber model. In the second calculation block, a plug flow reactor (PFR) (Levenspiel, 1999) model is used to simulate the co-current contact between aerosols and gas phase. Figure 1b represents the generic section 'i' of the model. Treated flue gas from section 'i' is mixed with the aerosols of section 'i+1' before entering PFR model. The outlet stream of PFR model at section 'i' is flashed to separate gas phase and aerosols before entering the next section 'i-i'. Rich solvent from section 'i-i' enters section 'i' as lean solvent. Similarly, treated flue gas from section 'i-i' is the inlet flue gas to section 'i'.

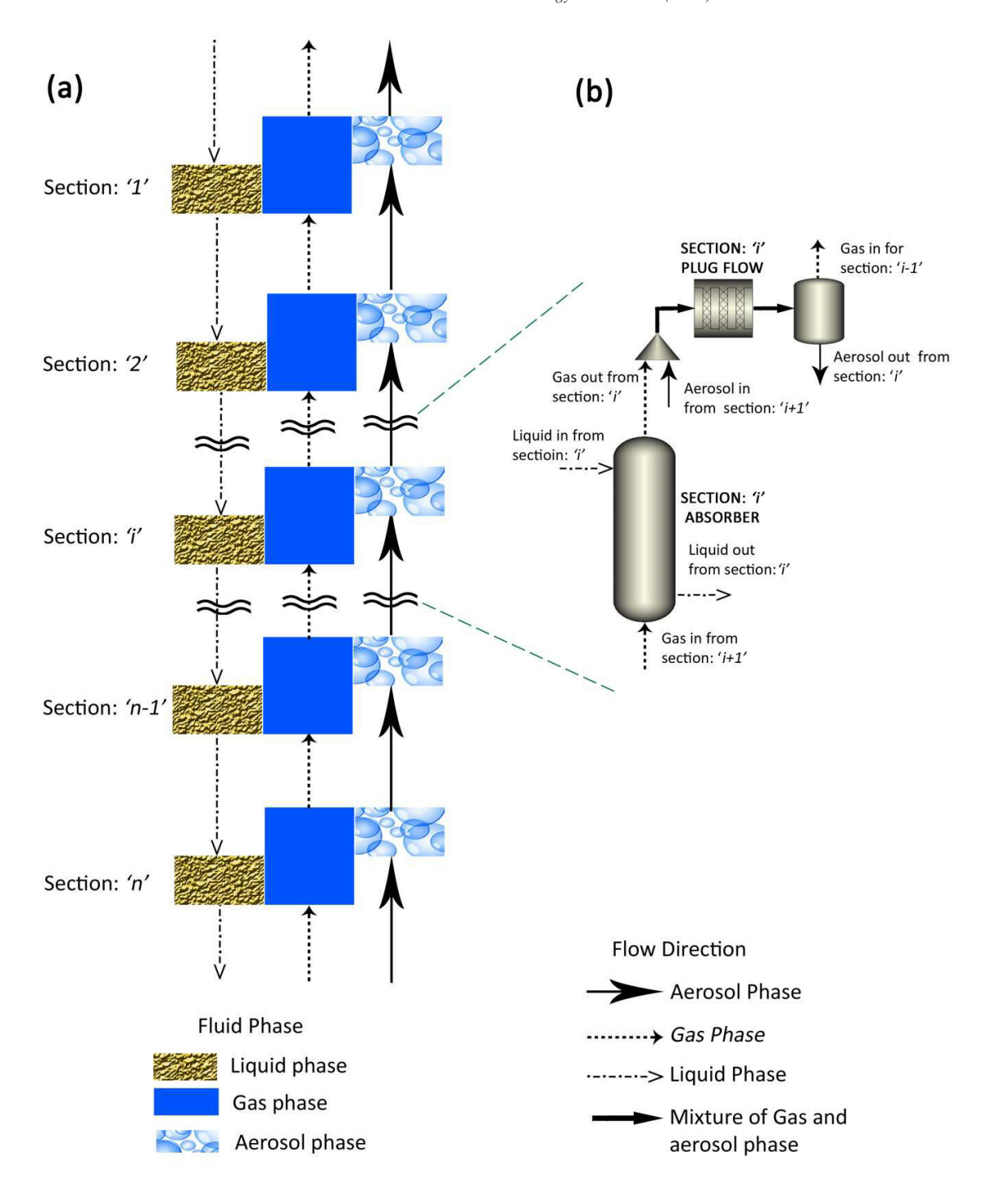


Figure 1. (a) Schematic representation of the modelling approach. Flue gas and aerosols enters the absorber section 'n' and lean solvent enter the absorber at section '1'; (b) Schematic representation of generic section 'i' as modelled in Aspen Plus. Aerosol phase and flue gas co-current mass and heat transfer process occurs in the Plug Flow Reactor. The solvent and flue gas counter current mass and heat transfer process occurs in the absorber column.

Table 1: Base Case - Inlet stream specification for the flue gas and the lean solvent.

Parameter	Flue gas	Solvent
Temperature (°C)	48	40
Flow rate (kg/sec)	616	2341
Pressure (bar)	1.016	1.016
Loading (mol CO <sub>2</sub> /mol MEA)	-	0.23
Composition		
Molecule	mole fraction (Flue gas)	mass fraction (Solvent)
$H_2O$	0.1127	0.655
MEA	-	0.295
$CO_2$	0.133	0.05
$N_2$	0.7162	-

0.0381

Table 2: Aspen Plus model equipment specification.

 $O_2$ 

Parameter	Value		
Absorber (each section)			
Packing type (-) Packing material (-)	Norton IMTP (50 mm) Metal		
Absorber total height (m)	20		
Absorber diameter (m)	21		
Absorber sectional height (m)	2		
Sectional Packing height (m)	2		
Packing diameter (m)	21		
Stages (-)	2		
Plug Flow Reactor			
Length (m)	2		
Diameter (m)	21		

The dimensions (length and diameter) of the PFR are similar to that of the absorber column. The PFR and flash drum operates at the same temperature and pressure as the gas phase. To demonstrate the discretization method and to quantify the aerosol based emission, a base case was defined as follows,

- An absorber column with a packing height of 20 m and 21 m diameter is divided into 10 sections with height of 2 m each
- A 90 % CO<sub>2</sub> removal from the flue gas
- A 30 MEA wt. % absorption liquid
- Lean loading of 0.23 mol CO<sub>2</sub>/mol MEA

The flue gas flow rate and composition for 600 MWe coal fired power plant (Abu-Zahra et al., 2007) is considered for this study. Table 1 shows the flow rate and composition of flue gas and lean solvent. Table 2 and the specifications of absorber model used in Aspen Plus. The corresponding liquid to gas ratio (L/G) is 3.5 kg of liquid/kg of gas.

A rate based absorber model (Rad Frac is the rate based model frame work in Aspen Plus) is used. The Electrolyte - NRTL (ELECNRTL) model in Aspen Plus is used to describe the thermodynamic property of the given

H<sub>2</sub>O-MEA-CO<sub>2</sub> system. The chemical reactions kinetics (MEA REA in Aspen Plus V8.0) considered for absorber and PFR model (Abu-Zahra et al., 2007, Zhang Y, and Chen C-C., 2013) are as shown in Table 3.

Table 3: Solution chemistry and kinetic reactions for MEA-CO<sub>2</sub>-H<sub>2</sub>O system.

Reaction name	Stoichiometry	
	Equilibrium	
Water Dissociation	$2 \text{ H}_2\text{O} \leftrightarrow \text{H}_3\text{O}^+ + \text{OH}^-$	
CO <sub>2</sub> hydrolysis	$CO_2 + 2 H_2O \leftrightarrow H_3O^+ + HCO_3^-$	
Bicarbonate dissociation	$HCO_3^- + H_2O \leftrightarrow H_3O^+ + CO_3^{-2-}$	
Carbamate Hydrolysis	$MEACOO^{-} + H_2O \leftrightarrow MEA + HCO_3^{-}$	
Amine Protonation	$MEA^{+} + H_{2}O \longleftrightarrow MEA + H_{3}O^{+}$	
Kinetic		
Carbamate formation	$MEA + CO_2 + H_2O \rightarrow MEACOO^- + H_3O^+$	
Bicarbonate formation	$CO_2 + OH^- \rightarrow HCO_3$	

The input parameters to the Aspen Plus model for the aerosols are inlet volume and composition and are calculated as follows:

- Step: 1. Assume a diameter for the aerosol droplet, say  $0.1 \mu m$ .
- Step: 2. Calculate the volume of a single aerosol by considering it as perfect sphere.
- Step: 3. Calculated volume in step 2 is multiplied with the aerosol number concentration to obtain the total volume of aerosol per m<sup>3</sup> gas phase.
- Step: 4. Multiply the value in step 3 with total volume of flue gas to obtain the inlet volume flow of aerosols in m<sup>3</sup>/s.
- Step:5. The sulphuric acid amount in the aerosols is calculated by multiply the expected sulphuric acid concentration (say 3 mg/Nm³) with the total gas volume

## 2.3. Assumptions

Several assumption have been used in order to simplify the modelling approach. They are as follows,

- 1. The aerosols number concentration is typically in the range of 10<sup>13</sup> to 10<sup>14</sup> per m<sup>3</sup> of gas (Khakharia et al., 2013). Here, the particle number concentration is assumed to be constant and equal to 10<sup>14</sup> per m<sup>3</sup> of gas, and the H<sub>2</sub>SO<sub>4</sub> concentration is assumed to be 3 mg/Nm<sup>3</sup>. Moreover, no coagulation or deposition of aerosols is considered.
- 2. The aerosol phase is modelled as bulk liquid phase
- 3. No nucleation in the absorber column (i.e. only growth of the aerosol is studied).
- 4. Chemical reactions take place only in liquid phase.
- 5. No direct contact between liquid phase and aerosols (i.e. mass and heat transfer process takes place only between the aerosols and gas phase).
- 6. The overall mass transfer of CO<sub>2</sub> and MEA is predominately liquid phase controlled. Therefore, the assumption can be made that surface area of the aerosols can be neglected.
- 7. The Kelvin effect is neglected. The vapour pressure for a curved surface will be larger than that of the flat surface. This increase in vapour pressure is described by Kelvin effect (Hinds, 2012).

$$\ln \frac{p}{p_0} = \frac{2\gamma V_m}{rRT}$$
 Eq. (2)

Here, p is the actual vapour pressure,  $p_0$  is the vapour pressure over a flat surface,  $\gamma$  is the surface tension,  $V_m$  is the molar volume of the liquid, r is the radius of the droplet, R is the universal gas constant, and T is the temperature. Small liquid droplets like aerosols will exhibit a higher effective vapour pressure, since the surface area is larger in comparison to the volume. As the size of the aerosols increases, the effective vapour pressure decreases and the droplets grow into bulk liquid. It can be easily verified using Eq. (2) that  $H_2O$  aerosols with a size larger than 25 nm in radius at any temperature above 30 °C, the vapour pressure over the curved surface will be equal to a flat surface *i.e.* the effect of surface curvature can be neglected. Therefore, in order to simplify the modelling approach the Kelvin effect is neglected.

#### 3. Results and discussion

In this section, some of the main parameters of the absorber section in a PCCC process will be studied as an initial step towards understanding aerosols based emission. Starting from the base case, the sensitivity of the following parameters on the aerosol based emissions is evaluated,

- CO<sub>2</sub> concentration in the inlet flue gas
- Lean solvent temperature
- Lean solvent loading (mol CO<sub>2</sub> / mol MEA)

By studying the impact of the above mentioned parameters on the supersaturation profile an insight into the mechanism of aerosol based emission can be obtained.

## 3.1. Base case

For the base case, the entire absorber column without discretizing into sections and no aerosols is simulated. The degree of supersaturation of the flue gas is calculated using Eq (1). Figure 2 shows the temperature and supersaturation profile across the absorber column. The temperature of the gas increases as the gas moves up the column due to the exothermic reaction between CO<sub>2</sub> and MEA. The temperature of the flue gas reaches its peak (i.e. hot zone), typically at 2/3 of the column for the chosen liquid to gas ratio. The increase in temperature along the column leads to increase in the partial pressure of volatile components such as water and MEA. This increase in partial pressure of the volatile components leads to an increase in the supersaturation ratio, however, remains below 1 until stage 2. Above the hot zone, the flue gas temperature decreases by the incoming relatively colder lean solvent. This results in a drastic decrease of the gas temperature forming a temperature bulge inside the absorber column. The temperature bulge can be defined as difference between maximum (hot zone) and top temperature of the flue gas in the absorption column.. The drastic temperature decrease leads to a crossover of the gas and liquid temperatures, with the gas being hotter than the liquid in stage 1 and 2. This leads to a significant increase in the supersaturation ratio and reaches a mximum of about 1.03 at the top of the column. Therefore, there is a potential for heterogeneous nucleation in the zone where S>1 resulting in the growth of aerosols by condensation of water and MEA. It can be inferred that reducing the difference between the gas and liquid temperatures, reduces the supersaturation ration and thereby, lowering the potential for aerosol formation.

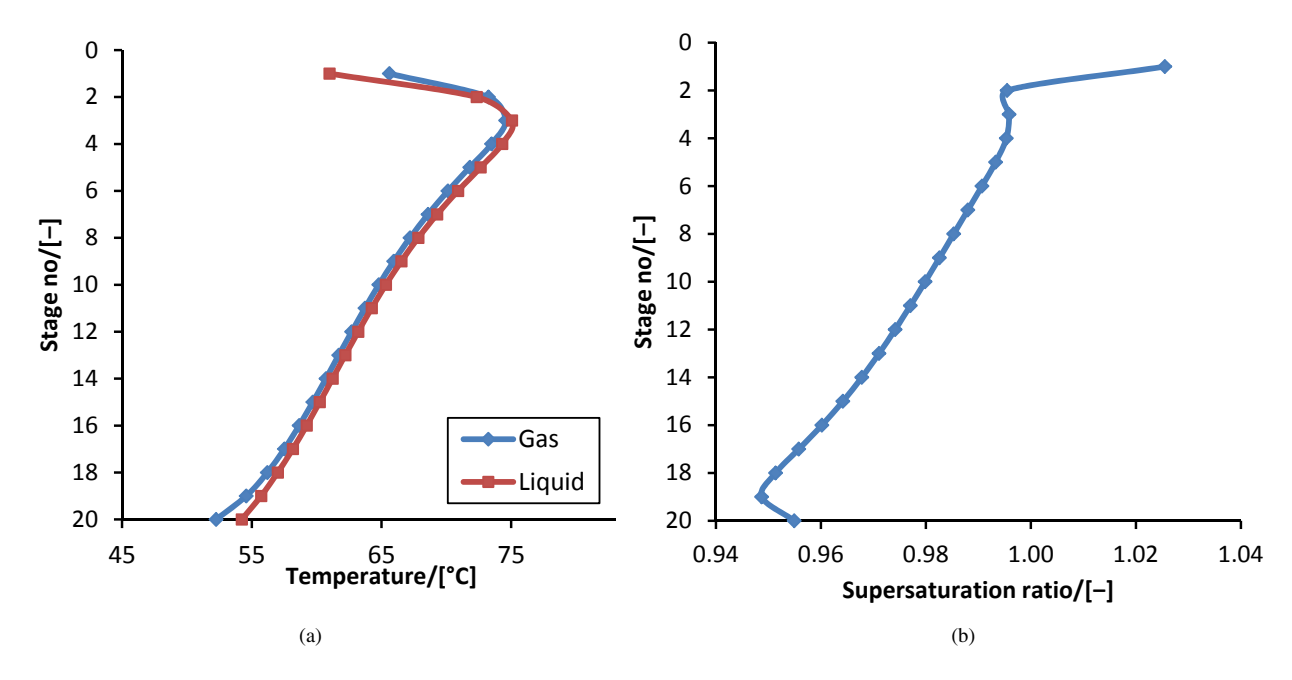


Figure 2. (a) Temperature profile and (b) Supersaturation profile along the absorber column for the case with no aerosols in the flue gas.

## 3.2. Effect of the change in inlet flue gas CO<sub>2</sub> concentration

The flue gas composition in terms of  $CO_2$  and  $O_2$  content of the power plant depends on factors like the composition of the fuel being burned, load variation, combustion conditions, etc. Moreover, studying the effect of different  $CO_2$  concentration in the flue gas gives an insight into the mechanism of aerosol based emissions.

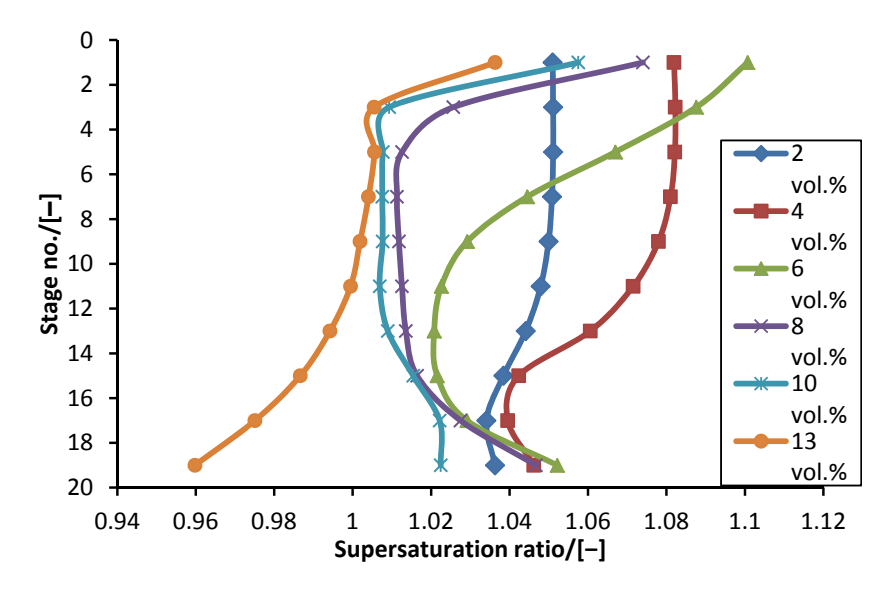


Figure 3. Supersaturation ratio along the absorber column for different concentration of CO<sub>2</sub> with aerosols in the inlet flue gas at a constant liquid to gas ratio.

The  $CO_2$  concentration in the flue gas is varied from 13 % to 2%, while the  $N_2$  concentration is adjusted to maintain a constant flow rate. The liquid to gas ratio is kept constant by maintaining the same liquid flow rate. From Figure 3, it can be observed that the supersaturation ratio along the column increases as the  $CO_2$  content is reduced. Moreover, at lower  $CO_2$  content the supersaturation ratio is greater than 1, even in the lower stages of the column. The supersaturation ratio has a maximum of 1.1 at 6 vol.%  $CO_2$  in the flue gas. Subsequently, the supersaturation ratio decreases on futher decrease in inlet  $CO_2$  content to 1.05 at 2 vol.%  $CO_2$ , but is still higher than the supersaturation ratio at 13 vol.%  $CO_2$ .

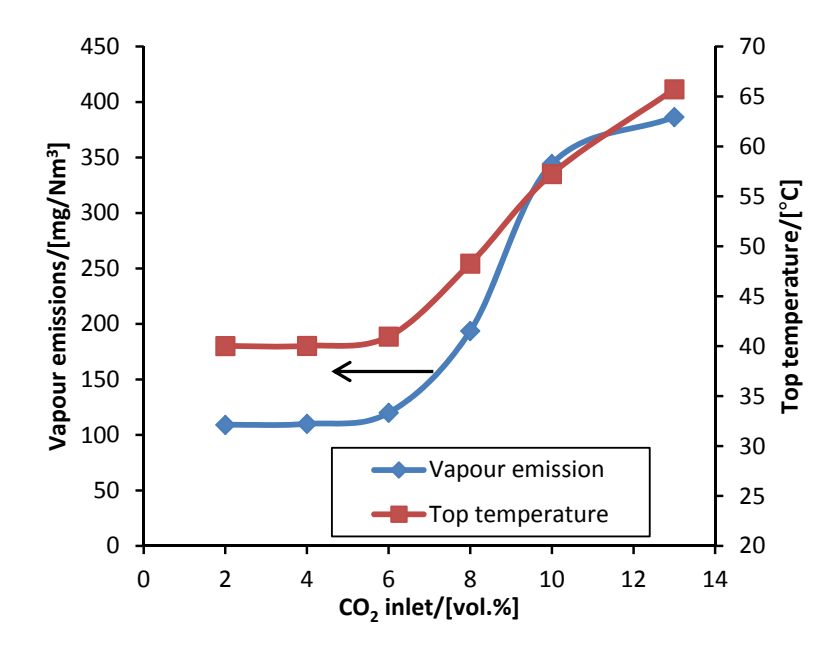


Figure 4. Temperature at the top of the absorber column and the corresponding vapour based emissions of MEA at varying inlet CO<sub>2</sub> content.

As seen in Figure 4, the temperature of the top stage in the absorber increases at higher CO<sub>2</sub> content because of the larger amount of higher amount of CO<sub>2</sub> transferred to the liquid phase, thereby increasing the total amount of heat released. This temperature increase causes the MEA content in the vapour stream leaving the absorber section to increase to a maximum of 386 mg/Nm<sup>3</sup> at 66 °C. The increase in vapour based emissions is in accordance with the corresponding increase in temperature and the expected change in activity of MEA in the solvent.

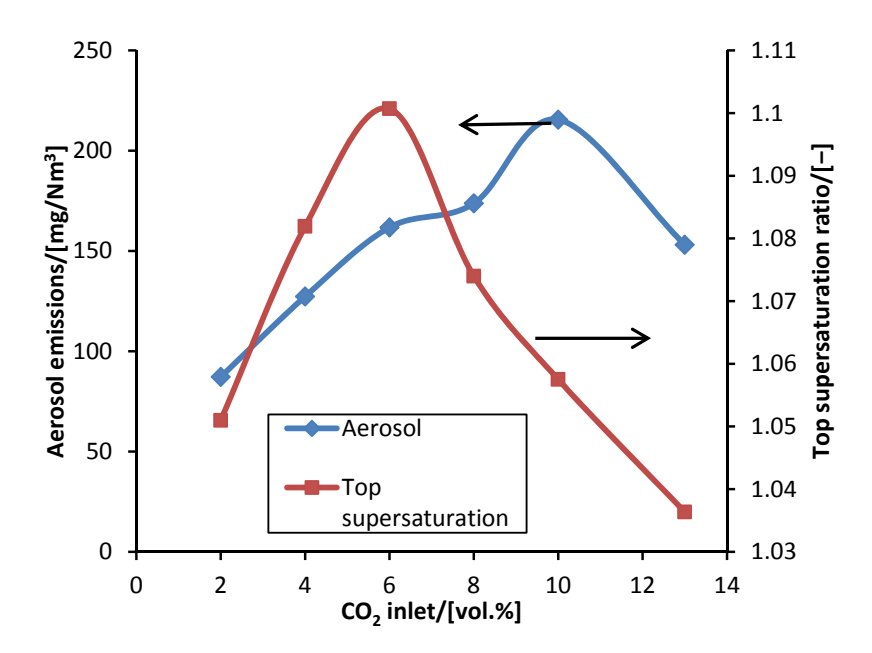


Figure 5. Supersaturation ratio at the top of the absorber column and the corresponding aerosol based emissions of MEA at varying inlet CO<sub>2</sub> content.

The supersaturation ratio at the top of the absorber column is maximum at 6 vol.% as seen in Figure 5. The aerosol based emissions are seen to increase from 80 mg/Nm³ to about 200 mg/Nm³ at 10 vol.% and reduces to 120 mg/Nm³ at 13 vol.% CO₂. The aerosol based emissions shows a maximum at 10 vol.% CO₂, unlike the maximum of supersaturation ratio at 6 vol.% CO₂. The aerosol based emission depends not only on the supersaturation ratio, but also on the absolute temperature at which the supersaturation occurs. The aerosol based emissions are expected to be higher if the concentration of volatile components in the gas phase available for transferring to the aerosol phase is higher at the same supersaturation ratio. This could be the possible cause of increase in aerosol based emissions from 6 to 10 vol.% CO₂. Moreover, the activity of the amine is an important parameter in determining the extent of volatile components present in the aerosol phase. As the activity of the MEA in the solvent reduces when the CO₂ content in the flue gas is increased, the aerosol based emissions reduces from 10 to 13 vol.% CO₂. As two competing effects; (i) increase in the volatile emissions and (ii) lowering of the amine activity, occur when the inlet CO₂ flue gas content is increased, the modelling methodology shows a mismatch between the top supersaturation ratio and corresponding aerosol based emissions.

## 3.3. Effect of the lean solvent temperature

In this case, the lean solvent temperature is varied from 30°C to 50°C, while keeping the remaining process parameters constant. On increasing the lean solvent temperature the flue gas temperature after the hot zone increases. Therefore, the temperature bulge decreases. The decrease in the temperature bulge decreases the top supersaturation ratio too, as shown in Figure 6.

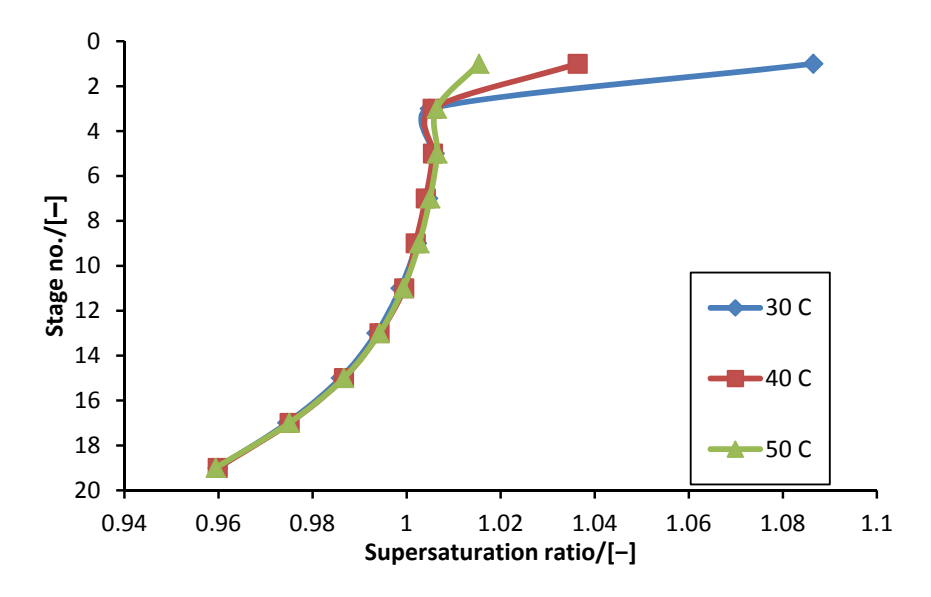


Figure 6. Supersaturation profile along the column at different temperatures of the lean solvent to the absorber.

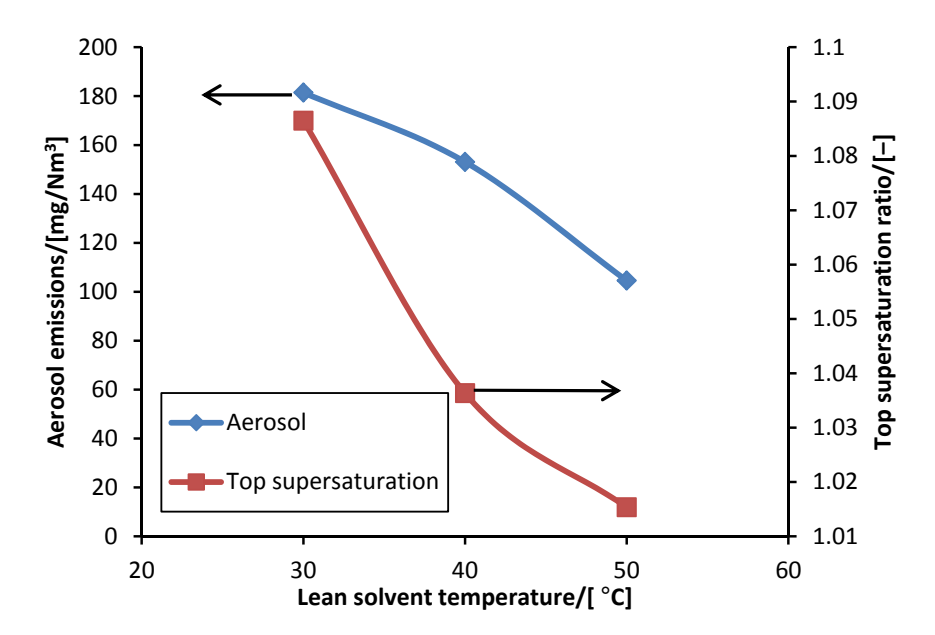


Figure 7. Aerosol based emission of MEA and top supersaturation ratio at varying temperature of the lean solvent to the absorber column.

The increase in the top supersaturation ratio results in higher aerosol based emission as shown in Figure 7. The top supersaturation ratio increases from 1.02 at 50 °C to 1.09 at 30°C, while the corresponding aerosol based emission increases from 105 to 181 mg/Nm³. However, the top temperature increase results in a higher vapour emission of MEA as shown in Figure 8. Therefore, the total emission increases on increasing the lean solvent temperature however, the aerosol based emission decreases. The high vapour emission can be more easily removed by a conventional wash section and therefore, increasing the lean solvent temperature can be a short-term solution for reducing aerosol based emissions.

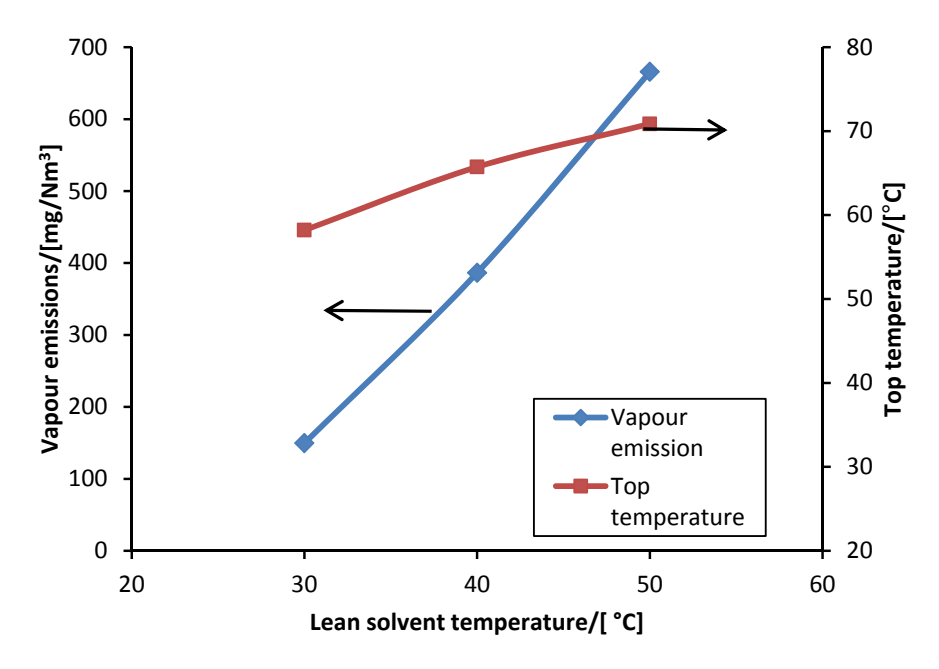


Figure 8. Vapour emissions of MEA and the top temperature at varying temperatures of the lean solvent to the absorber column.

## 3.4. Effect of the lean solvent loading

The lean solvent loading represents the degree of regeneration in the stripper. The lean loading of the solvent is varied from 0.13 to 0.30 mol  $CO_2$  / mol MEA at a constant liquid to gas ratio. Therefore, the  $CO_2$  capture percentage decreases as the  $CO_2$  loading of the lean solvent increases. As shown in Figure 9, the supersaturation profile increases, especially at the top of the column as the lean loading decreases. Up to a lean loading of 0.23, the supersaturation ratio at the bottom of the column is below 1, and increases throughout the column reaching a maximum at the top. However, as the lean loading decreases further, an additional zone of high supersaturation ratio is formed in the lower section of the column. As the lean loading of the solvent increases, the transfer of  $CO_2$  to the solvent shifts lower in the column. Therefore, majority of the corresponding heat is also released is in the lower sections of the column resulting in an increase in the supersaturation ratio in the lower section of the column. Moreover, the activity of the volatile components, MEA and water, also increases as the lean loading of the solvent is reduced.

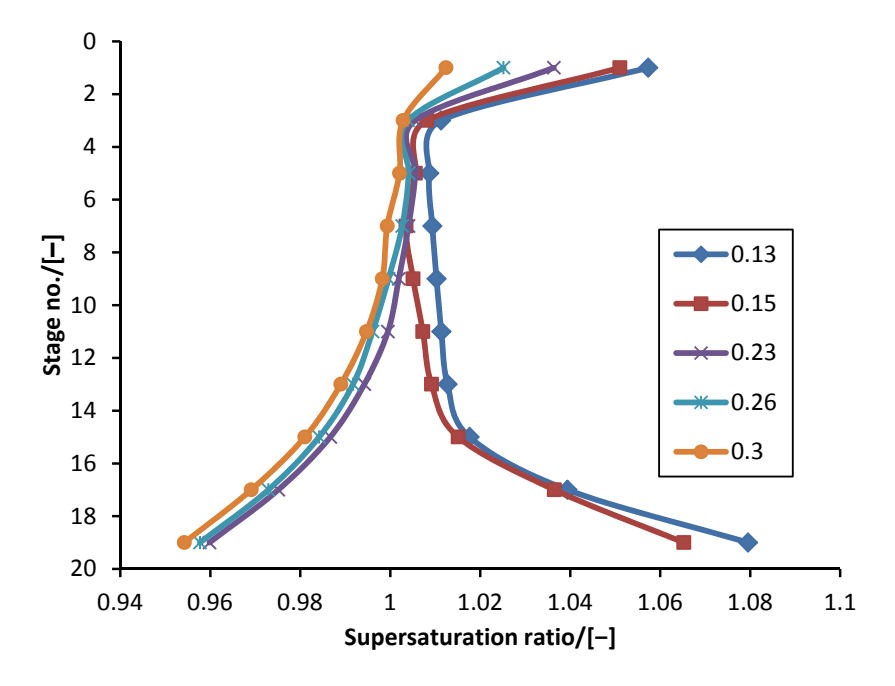


Figure 9. Supersaturation profile along the column at varying CO<sub>2</sub> loading of the lean solvent.

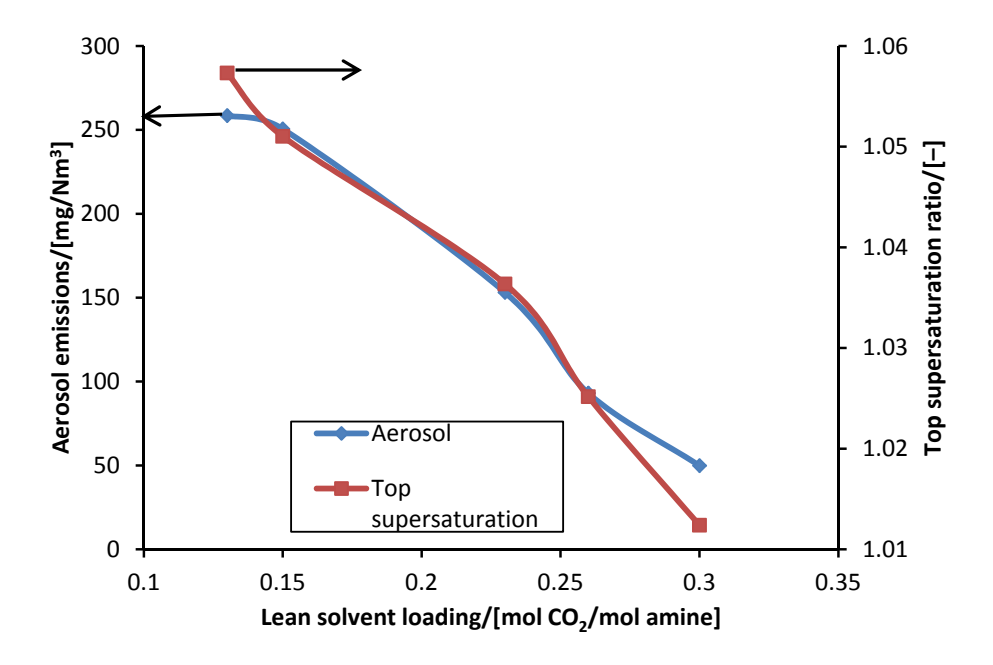


Figure 10. Aerosol based emission of MEA and the top supersaturation ratio in the absorber column for varying CO2 loading of the lean solvent.

The corresponding aerosol based emissions also reduces as the  $CO_2$  loading of the lean solvent is increased as shown in Figure 10. The lower supersaturation ratio at the top of the absorber column is a result of the lower activity of the volatile components at higher  $CO_2$  loading of the lean solvent. The top temperature in the absorber column

increases as the lean loading is reduced from 0.3 to 0.23. The corresponding vapour based emissions of MEA also increases as shown in Figure 11. On further decrease of the lean loading, most of the  $CO_2$  is transferred at the bottom sections of the column causing more cooling in the top section of the column and a lower top temperature. This is confirmed by the supersaturation profile change as shown in Figure 9. However, the corresponding MEA vapour emission is seen to increase as a result of it higher activity in the solvent and reduces, only at the lean loading of 0.13. Therefore, increasing the lean loading of the solvent decreases the aerosol based as well as total emissions.

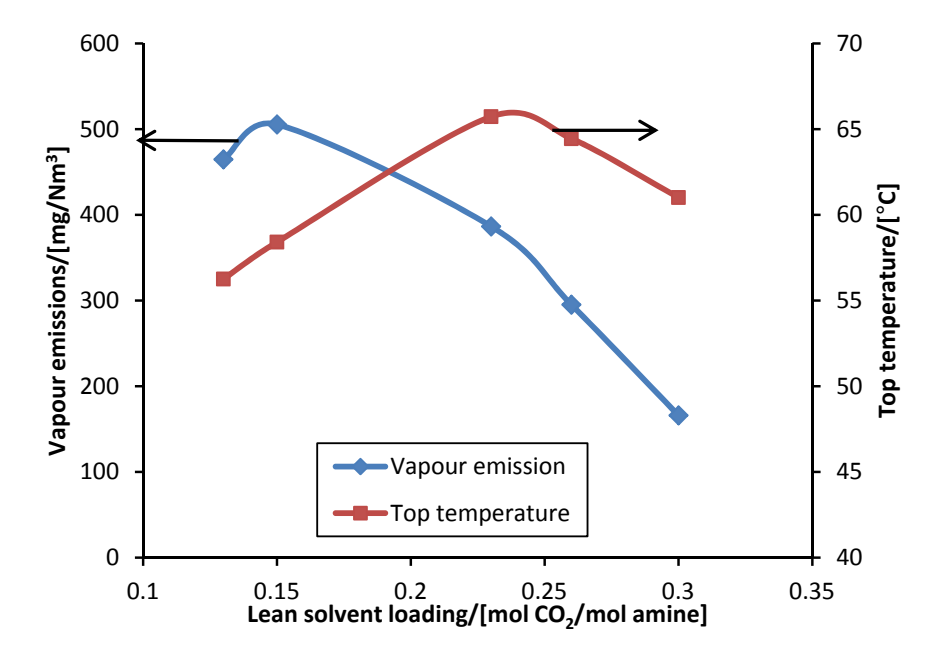


Figure 11. Vapour emissions of MEA at the corresponding top temperature in the absorber column for varying CO<sub>2</sub> loading of the lean solvent.

## 4. Results and discussion

Aerosol based emissions of solvent and its components from a PCCC plant need to be understood in detail from both an experimental and theoretical perspective. In this study, a simplified methodology has been presented for understanding aerosol based emissions from a CO<sub>2</sub> capture absorber column in a PCCC process. The degree of supersaturation was found to be an important parameter in predicting the extent of the aerosol based emissions. The impact of various process parameters such as the inlet flue gas CO<sub>2</sub> concentration, the temperature of the lean solvent and the CO<sub>2</sub> loading of the lean solvent, on supersaturation profile along the column was investigated. Increasing the lean solvent temperature and the lean solvent loading resulted in lowering of the aerosol based emissions. A maximum in the supersaturation ratio was observed at 6 vol.% CO<sub>2</sub> and the maximum in aerosol based emissions was observed at 10 vol.% CO<sub>2</sub>. The mismatch in the maximum of aerosol based emissions and top supersaturation ratio is possibly due to the methodology being not suited for two competing mechanisms. In general, the aerosol based emissions followed the trend of the supersaturation ratio at the top of the absorber column. The methodology presented in this study can be used for predicting aerosol based emissions with solvents other than MEA and in reactive absorption processes. Future research on this topic is directed towards comparing the model results with experiments and thereby, validate the model.

#### Acknowledgements

This work has been partially sponsored by the CATO2 program (http://www.co2-cato.org). The authors would like to thank Viknesan Ganesan for his contribution.

#### References

- [1] Aaheim, H.A., Kristin, A., Seip, H.M., 1999. Climate change and local pollution effects—an integrated approach. Mitig. Adapt. Strateg. Glob. Change 4, 61–81.
- [2] Abu Zahra, M.R.M., 2009. Carbon dioxide capture from flue gas: development and evaluation of existing and novel process concepts. (Phd Thesis). Technical University of Delft, The Netherlands.
- [3] Abu-Zahra, M.R.M., Schneiders, L.H.J., Niederer, J.P.M., Feron, P.H.M., Versteeg, G.F., 2007. CO2 capture from power plants. Int. J. Greenh. Gas Control 1, 37–46.
- [4] Abunowara, M., Elgarni, M., 2013. Carbon Dioxide Capture from Flue Gases by Solid Sorbents. Energy Procedia 37, 16-24.
- [5] Alie, C., Backham, L., Croiset, E., Douglas, P.L., 2005. Simulation of CO2 capture using MEA scrubbing: a flowsheet decomposition method. Energy Convers. Manag. 46, 475–487.
- [6] Brachert, L., Mertens, J., Khakharia, P., Schaber, K., 2014. The challenge of measuring sulfuric acid aerosols: Number concentration and size evaluation using a condensation particle counter (CPC) and an electrical low pressure impactor (ELPI+). J. Aerosol Sci. 67, 21–27.
- [7] Da Silva, E.F., Kolderup, H., Goetheer, E., Hjarbo, K.W., Huizinga, A., Khakharia, P., Tuinman, I., Mejdell, T., Zahlsen, K., Vernstad, K., Hyldbakk, A., Holten, T., Kvamsdal, H.M., van Os, P., Einbu, A., 2013. Emission studies from a CO2 capture pilot plant. Energy Procedia 37, 778–783.
- [8] De Koeijer, G., Enge, Y., Sanden, K., Graff, O.F., Falk-Pedersen, O., Amundsen, T., Overå, S., 2011. CO2 Technology Centre Mongstad–Design, functionality and emissions of the amine plant. Energy Procedia 4, 1207–1213.
- [9] Gretscher, H., Schaber, K., 1999. Aerosol formation by heterogeneous nucleation in wet scrubbing processes. Chem. Eng. Process. Intensif. 38, 541–548.
- [10] Hinds, W.C., 2012. Aerosol Technology: Properties, Behavior, and Measurement of Airborne Particles. John Wiley & Sons.
- IEAGHG, 2010. Environmental Impacts of Amine Emissions During Post Combustion Capture. Rep. No 201011 2010.
- [11]Khakharia, P., Brachert, L., Mertens, J., Huizinga, A., Schallert, B., Schaber, K., Vlugt, T.J.H., Goetheer, E., 2013. Investigation of aerosol based emission of MEA due to sulphuric acid aerosol and soot in a Post Combustion CO2 Capture process. Int. J. Greenh. Gas Control 19, 138–144.
- [12] Khakharia, P., Huizinga, A., Jurado Lopez, C., Sanchez Sanchez, C., de Miguel Mercader, F., Vlugt, T.J.H., Goetheer, E., 2014a. Acid Wash Scrubbing as a Countermeasure for Ammonia Emissions from a Postcombustion CO 2 Capture Plant. Ind. Eng. Chem. Res. 53, 13195–13204.
- [13] Khakharia, P., M Kvamsdal, H., da Silva, E.F., Vlugt, T.J.H., Goetheer, E., 2014b. Field study of a Brownian Demister Unit to reduce aerosol based emission from a Post Combustion CO<sub>2</sub> Capture plant. Int. J. Greenh. Gas Control 28, 57-64.
- [14] Levenspiel, O., 1999. Chemical reaction engineering. Wiley, New York.
- [15] MacDowell, N., Florin, N., Buchard, A., Hallett, J., Galindo, A., Jackson, G., Adjiman, C.S., Williams, C.K., Shah, N., Fennell, P., 2010. An overview of CO2 capture technologies. Energy Environ. Sci. 3, 1645–1669.
- [16] Mertens, J., Knudsen, J., Thielens, M.-L., Andersen, J., 2012. On-line monitoring and controlling emissions in amine post combustion carbon capture: A field test. Int. J. Greenh. Gas Control 6, 2–11.
- [17] Mertens, J., Lepaumier, H., Desagher, D., Thielens, M.-L., 2013. Understanding ethanolamine (MEA) and ammonia emissions from amine based post combustion carbon capture: Lessons learned from field tests. Int. J. Greenh. Gas Control 13, 72–77.
- [18] Min, S.-K., Zhang, X., Zwiers, F.W., Hegerl, G.C., 2011. Human contribution to more-intense precipitation extremes. Nature 470, 378–381.
- [19] Mori, S., Miyaji, K., Kamegai, K., 2013. CCS, Nuclear Power and Biomass An Assessment of Option Triangle under Global Warming Mitigation Policy by an Integrated Assessment Model MARIA-23. Energy Procedia 37, 7474–7483.
- [20] Nguyen, T., Hilliard, M., Rochelle, G., 2011. Volatility of aqueous amines in CO2 capture. Energy Procedia 4, 1624-1630.
- [21] Nguyen, T., Hilliard, M., Rochelle, G.T., 2010. Amine volatility in CO2 capture. Int. J. Greenh. Gas Control 4, 707-715.
- [22] Rao, A.B., Rubin, E.S., 2002. A Technical, Economic, and Environmental Assessment of Amine-Based CO<sub>2</sub> Capture Technology for Power Plant Greenhouse Gas Control. Environ. Sci. Technol. 36, 4467–4475.
- [23] Rochelle, G.T., 2009. Amine Scrubbing for CO2 Capture. Science 325, 1652-1654.
- [24] Sanchez-Fernandez, E., Mercader, F. de M., Misiak, K., van der Ham, L., Linders, M., Goetheer, E., 2013. New Process Concepts for CO2 Capture based on Precipitating Amino Acids. Energy Procedia 37, 1160–1171.
- [25] Schaber, K., 1994. Aerosol formation in absorption processes. Chem. Eng. Sci. 50, 1347-1360.
- [26] Seader, J.D., Henley, E.J., Roper, D.K., 2010. Separation Process Principles. Wiley.
- [27] Srivastava, R.K., Miller, C.A., Erickson, C., Jambhekar, R., 2004. Emissions of Sulfur Trioxide from Coal-Fired Power Plants. J. Air Waste Manag. Assoc. 54, 750–762.
- [28] Trollebø, A.A., Saeed, M., Hartono, A., Kim, I., Svendsen, H.F., 2013. Vapour-Liquid Equilibrium for Novel Solvents for CO2 Post Combustion Capture. Energy Procedia 37, 2066–2075.
- [29] Wall, T.F., 2007. Combustion processes for carbon capture. Proc. Combust. Inst. 31 I, 31–47.
- [30] Wattanaphan, P., Sema, T., Idem, R., Liang, Z., Tontiwachwuthikul, P., 2013. Effects of flue gas composition on carbon steel (1020) corrosion in MEA-based CO2 capture process. Int. J. Greenh. Gas Control 19, 340–349.
- [31] Yildirim, Ö., Kiss, A.A., Hüser, N., Leβmann, K., Kenig, E.Y., 2012. Reactive absorption in chemical process industry: A review on current activities. Chem. Eng. J. 213, 371–391.
- [32] Zhang Y, and Chen C-C., 2013. "Modelling CO2 absorption and desorption by aqueous monoethanolamine solution with Aspen rate-based model, Energy Procedia, 1584-1596.